Arab J. Nucl. Sci. Appl., Vol. 58, 4, 29-49 (2025)

ISSN 1110-0451

Arab Journal of Nuclear Sciences and Applications

Web site: ajnsa.journals.ekb.eg

(E S N S A)

Optimizing CDMA Performance for Harsh Wireless Channels: Energy Adaptation and Predictive BER Analysis for Nuclear Communication Environments

Elsayed H. Ali[1], Mohamed S. El-Tokhy[1], H. Kasban[1] and Ibrahim M. Fayed[2]

[1]*Engineering Department, Nuclear Research center (NRC), Egyptian Atomic Energy Authority (EAEA), Egypt*
[2]*Network Planning Department, National Telecommunication Institute, Egypt*

ARTICLE INFO

Article history:

Received: 11th July 2025
Accepted: 9th Sept. 2025
Available online: 21st Sept. 2025

Keywords:

Wireless Communication Systems,
CDMA, Mean Transmitter Energy Gain (MTEG),
Bit Error Rate (BER),
Adaptive Power Control,
Fading Channels, Nuclear Environment,
Non-Gaussian Noise.

ABSTRACT

This manuscript presents a comprehensive framework for optimizing Code Division Multiple Access (CDMA) performance in harsh wireless channels, with a specific focus on nuclear communication environments characterized by severe, non-Gaussian noise. We propose and derive novel closed-form analytical expressions for two critical Quality of Service (QoS) parameters: Mean Transmitter Energy Gain (MTEG) and Bit Error Rate (BER), under generalized fading conditions, including Exponential, Weibull, and Nakagami-m distributions. Our analysis identifies an optimal operating point, revealing that the MTEG is minimized at a channel degradation of 0.2 dB, representing a crucial trade-off between energy efficiency and transmission robustness. For error performance, the average and predicted BER are rigorously analyzed, demonstrating that the number of subcarriers has a negligible impact on BER at a Signal-to-Noise Ratio (SNR) of 1 dB, while performance is significantly influenced by modulation constants and fading parameters. A key finding is the consistent superiority of uncoded CDMA over its coded counterpart in the studied interference-limited regime. To bridge the gap between theory and practice, we extend the analysis to real-world nuclear industrial settings by transmitting experimentally acquired signals Residence Time Distribution (RTD) curves and gamma scanning profiles using CDMA schemes. These empirical signals, measured via scintillation detectors, introduce structured, non-Gaussian noise that deviates profoundly from standard Additive White Gaussian Noise (AWGN) and Rayleigh fading assumptions. Comparative results across BPSK, QPSK, and 16QAM modulations, with and without convolutional coding, demonstrate that while real nuclear noise degrades performance, adaptive strategies informed by our models can maintain reliability.

1. INTRODUCTION

The most important issue in the design and investigation of broadband wireless communication systems in the future consists of support to a wide range of services and high data bit rates [1-3]. Hence, the significant interest for transmission with super data rates using wireless channels forwarded the progress of MCCDMA using multi-input multi output systems for subsequent generation of data communication[4-6]. Furthermore, MC-CDMA scheme is supposed to be the mainly chief future technique of wireless systems [6-8]. This technology has several characteristics and merits such as improved spectral efficiency, robustness to frequency selective channels, narrow band, vast bandwidth and multiple access ability [9-12]. Moreover, it offers soft handover, enhanced spectrum efficiency and simplified frequency planning [13-15]. This paper investigates the performance of CDMA systems with energy harvesting nodes. The nodes harvest energy from the ambient environment and use it to transmit data. The paper proposes an energy-efficient power allocation algorithm that takes into account the energy harvesting rate and the channel quality. MC-CDMA has digital modulation technique. Also, it is figured as multi-carrier system in which merges two technologies in order to improve the communication efficiency [2, 16, 17]. These technologies represent OFDM and CDMA [18-21]. CDMA is employed in many applications and becomes

Corresponding author: sayedmahdy@yahoo.com
DOI: 10.21608/ajnsa.2025.402798.1892

the subject of much research because of the various advantages it offers when employed in the cellular communication environment. The benefits include the ability to operate asynchronously in multiple access channels while tolerating the interference generated by other users [2, 22]. CDMA has multiple accesses. It is an interference limited system. Contrary, the increased numbers of users deteriorate the system efficiency [23, 24]. Accordingly, the beginning of extra users for CDMA leads to very graceful performance degradation, a distinctive advantage over the FDMA and TDMA systems [18, 21, 25-27]. CDMA depends on spread spectrum signalling. It is a considerable multiple-access technique. Orthogonality is established between subcarriers. It is the basic property of CDMA system that facilitating to combat the channel-fading phenomenon and to avoid narrowband interference in multi access technologies [9, 28]. Power limitation is the central restriction in various transceivers of wireless schemes and user terminals. The common power allocation problem corresponds to correlation between best BER and restriction of all power transmission power [9, 28]. Uplink (MS to BTS) and downlink (BTS to MS) in a CDMA system have different characteristics that must be individually examined [29]. Uplink is used for setting the coverage. But, downlink is employed for estimating number of users [25, 27]. Fading induced attenuation is a common problem with channels of wireless channels [30]. Atmospheric surroundings between transmitter and receiver have great influence on channel performance. Atmospheric turbulence is uncontrolled conditions. It leads to fast fluctuations on received signal. Hence, the transmitting signal gain of channel can be destroyed [31, 32]. The continuous break of attenuated signal will not allow the receiver to estimate transmitted signal [18]. Consequently, QoS in mobile network appeared as obstacle with applications of multimedia traffic [27, 33, 34]. A key problem in system design ensures transmission of data to all users, within the required QoS parameters [20, 35]. The major QoS parameters of interest are mean transmitter energy gain and BER [21, 36]. Part of the implemented work is an extension to that implemented in [37-39]. Overall, the literature shows that energy adaptation and power allocation are important techniques for improving the performance of CDMA wireless communication networks. Adaptive algorithms that take into account the channel quality and the desired QoS parameters can achieve better performance in terms of outage probability and average BER compared to fixed allocation methods. Energy-efficient power allocation algorithms that consider the energy harvesting rate and channel estimation error can also improve the energy efficiency of CDMA systems. This paper proposes an energy-efficient power allocation algorithm for DS-CDMA systems with imperfect channel state information. The algorithm takes into account the channel estimation error and the desired QoS parameters to allocate the transmit power of each user. Simulation results show that the proposed algorithm achieves a better performance in terms of energy efficiency and outage probability compared to traditional power allocation methods. The contents of such paper are as follows: system description is characterized in Section 2. The MTEG is analyzed in Section 3. As well, error investigation is offered in Section 4. Discussion of the results is introduced in Section 5. Section 6 is devoted to conclusion of the work.

2. SYSTEM PRELIMINARY

2.1. Transmitted signal

In this manuscript, the analysis and evaluation of the performance of CDMA is the main focus. Specifically, the authors examine the transmitter energy adaptation and error analysis under channel fading. To achieve this, the authors make use of a transmitter model found in [17, 36], which assumes a MIMO MC DS-CDMA system with K users. The system also makes use of multiple carrier direct sequence of CDMA technology with transmitted antennas (Mt) and received antennas (Nr). The authors assume that the CTI known at receiver establishes the system operation, and the transmitter depends on STBC to allow transmit diversity by receiver. The transmission process involves converting serial input data to parallel U sub-streams, with the symbols in each sub-stream being spread in time domain and mapped to Mt. Every subcarrier is a multicarrier signal modulated using inverse fast Fourier Transform (IFFT), and the modulated signals are then summed up and transmitted. The authors also assume that the communication channel between transmitter and receiver has frequency non-selective multiple fading. They investigate the performance of the system through an algorithm for energy adaptation that is implemented to overcome degradations of the received signal. The authors observe that the optimum variation for MTEG is achieved at channel degradation of 0.2dB. The authors also analyze the average bit error rate (BER) and predicted error rate of CDMA under channel impairments. They find that the number of subcarriers has no influence on BER at SNR of 1dB, but a shift in

the peak value of BER is noticed under the variation of modulation constant and fading parameters. The comparison between coded and uncoded CDMA confirms the superiority of uncoded CDMA. Finally, the authors investigate how the performance characteristics of CDMA are influenced by the variation of average SNR, rate of punctured code, and minimum free distance, which they evaluate through proposed closed-form expressions to achieve higher CDMA performance. A transmitter model is found in [18, 40]. It is supposed that transmitter has K users. The users channel in MIMO MC DS-CDMA system. Multiple carrier direct sequence of CDMA technology with transmitted antennas (M_t) and received antennas (N_r) is assumed. The CTI known at receiver establishes the system operation. Transmitter depends on STBC to allow transmit diversity by receiver. Firstly, serial input data are converted to parallel U sub-streams. Subsequently, the symbols in each sub-stream are spread in time domain that mapped to M_t. Therefore, every subcarrier is a multicarrier signal modulated by using IFFT. Then, the summation of the modulated signals is carried out and transmitted. Additionally, the communication channel between transmitter and receiver with frequency non-selective multiple fading is of primary assumption.

2.2. Channel phenomena

The wireless channel through which signals are transmitted is often subject to various phenomena that can degrade signal quality. One common issue is multipath fading, which occurs when the signal is reflected off of different surfaces and takes multiple paths to reach the receiver. This can cause fluctuations in the phase, angle of arrival, and amplitude of the received signal, leading to signal degradation. To accurately predict the impact of fading on the signal, models such as Weibull, chi-square, Nakagami-m, exponential, and Rayleigh fading distributions are often used to reduce its effects. In this manuscript, the complex low pass declarations for the Kth users in the wireless channel are given by equation (1). The wireless channel is supposed to have multipath frequency selective. The declarations of complex low pass for K^{th} users can be declared by [41]

$$h_k(t) = \sum_{l=0}^{L_p-1} \beta_{kl}\,\delta\left(t-\tau_{kl}\right)e^{j\eta_{kl}} \qquad (1)$$

where β_{kl}, τ_{kl} and η_{kl} denote the l^{th} path gain, delay and phase for the k^{th} user, respectively. The signal travels in any wireless communication channel from transmitter to receiver over multiple paths. It causes fluctuations in phase, angle of arrival and amplitude of the received signal. Therefore, it gives rise to multipath fading. The accurate prediction of fading influence needs a model to reduce such impacts in wireless channel [19, 21]. Thus, the link between M_t transmitter antennas and N_r receiving antennas is supposed to be subjected to Weibul, chi-square, Nakagami-m, exponential and Rayleigh fading distributions.

2.3. Receiver detected signal

The MC DS-CDMA technology with orthogonal MIMO serves K asynchronous users CDMA active users communicating with the base station in a single cell is considered. Too, the number of subcarriers is initiated to be equal to spreading factor. Besides, every subcarrier signal is assumed to experience a fading. Furthermore, it is supposed that the average powers received from all users at the BS are equal. The receiver model in [22, 27, 42] is employed. Afterwards, demodulation of received signal is performed by FFT based multicarrier demodulation in order to obtain U number of parallel flows that stands for transmission of U subcarriers. What's more, the considered streams are supposed to be space time that dispread in order to make decision variable for any of transmitted data bits. Accordingly, combining and detection of the received signals are carried out. Lastly, parallel to serial conversion is executed to yield output data [16, 21, 41, 43].

Step 1	**Generate a Binary Code by Mobile Station**
Step 2	**Modulate the Generated Code by a Modulator**
Step 3	**Do a Control on Transmitter Power**
Step 4	**Transmit the Signal through a Communication Channel**
Step 5	**Measure the Transmitted SNR by Receiver Base Station**
Step 6	**Send a Signal to Transmitter Power Control for Readjusting the Transmitted Power**

Fig. (1): Variable energy adaptation algorithm [3]

3. MEAN TRANSMITTER ENERGY GAIN

MTEG is a key parameter in evaluating the performance of CDMA systems. It is defined as the ratio of the average power transmitted by all users to the average power transmitted by a single user. In other words, it is the average energy gain of the transmission system due to the use of multiple users transmitting simultaneously. The MTEG value can be optimized to improve the overall performance of the system. An algorithm for energy adaptation is implemented to adjust the MTEG value to overcome degradations of the received signal due to channel impairments such as fading. The optimum variation for MTEG is observed at a channel degradation of 0.2dB. By adjusting the MTEG, the transmission system can better handle channel impairments and improve overall performance. The user power depends on adapting the transmitter energy. Though, the variable energy adaptation (VEA) is necessary for reduction and compensation of the interference with other cells. So, the CDMA system is enhanced alongside variants of fading channel [3, 44]. However, the user energy is related to the channel conditions. The user energy is increased to compensate the interference from neighbouring cells in the case of bad channel. But, it remains fixed in the case of good channel. Therefore, the lowest signal interference is achieved. On other hand, a better QoS is obtained. Mobile station (MS) generates a binary code that modulated and transmitted through CDMA channel. The power of MS is adapted according to the measured SNR by base station. The communication channel is noisy. Therefore, the transmitted data may be corrupted. Overcoming these shortcomings is the main objective of the receiver. As a consequence, a message is submitted from BS to MS for adaptation of transmitted power. The VEA algorithm is presented in Fig. 1 [3]. The VEA algorithm corresponds to adaptive modulation technique to increase the average throughput of the system by switching between modes of modulation relying on channel quality [3, 30]. So, higher amount of bits per symbol will be transmitted over high order modulation as the channel quality is of concern. But, the error probability is reduced by switching of modulated modes to lower order as the channel is hostile [30].

The steps in Figure (1) is explained in details as follows. Step 1: Generate a Binary Code by Mobile Station The first step in the process of wireless communication is the generation of a binary code by the mobile station. The binary code represents the information that the mobile station wants to transmit. Step 2: Modulate the Generated Code by a Modulator In the second step, the binary code generated by the mobile station is modulated by a modulator. Modulation is the process of converting the binary code into a format that can be transmitted over a wireless channel. The modulator typically uses a carrier wave to transmit the binary code. Step 3: Do a Control on Transmitter Power In the third step, the transmitter power is controlled. The transmitter power is adjusted to ensure that the transmitted signal has the appropriate strength for the wireless channel. This step is important to ensure that the signal is not too weak or too strong, which can result in poor communication quality or interference with other wireless devices. Step 4: Transmit the Signal through a Communication Channel In the fourth step, the modulated signal is transmitted through a communication channel. The communication channel can be wireless or wired. In the case of wireless communication, the signal is transmitted through the airwaves. Step 5: Measure the Transmitted SNR by Receiver Base Station In the fifth step, the receiver base station measures the SNR of the transmitted signal. SNR is a measure of the strength of the transmitted signal compared to the background noise. This step is important to ensure that the transmitted signal can be properly decoded at the receiver end. Step 6: Send a Signal to Transmitter Power Control for Readjusting the Transmitted Power In the final step, the receiver base station sends a signal to the transmitter power control to readjust the transmitted power.

Furthermore, our analysis reveals the existence of an optimum value for the fading parameter that minimizes the MTEG, a finding that is robust across the fading models studied. This optimum, observed at $\lambda=0.2\lambda=0.2$ dB for the exponential fading model, represents a critical balance between the need for adaptive energy expenditure and the inefficiency of operating at the maximum power limit. The existence of this optimum provides a valuable design guideline for maximizing the energy efficiency of adaptive transmission systems in fading environments.

The transmitted power is readjusted to improve the SNR of the signal at the receiver end. This step is important to ensure that the communication quality is maintained throughout the transmission. The MTEG refers to reduced average energy-to-noise ratio (ESR)

from the required energy-to-noise ratio using a non-adaptive system. It is given by [37, 45]

$$MTEG = \frac{R_{Max}}{\langle R \rangle} \quad \textbf{(2)}$$

where R, R_{max} and <.> denote the transmitted energy-to-noise ratio, maximum value of R and mean value, respectively.

The detected signal ENR is stated as [37]

$$\frac{E(t)}{N_0} = R\,\frac{a^2(t)}{2} \quad \textbf{(3)}$$

The a(t) refers to the received signal amplitude. Its density function is corresponding to exponential fading channel. It is assumed that $\Psi(y)=E(t)/N_0$. The CDF of $\frac{a^2}{2}$ under exponential channel fading is given by

$$F_{\frac{a^2}{2},Exp}\left(\frac{\Psi(y)}{R}\right) = 1 - e^{-\lambda\Psi(y)} \quad \textbf{(4)}$$

where λ is exponential fading parameter. The differentiation of Eq. (4) with respect toyields $\Psi(y)$

$$\frac{1}{R} f_{\frac{a^2}{2},Exp}\left(\frac{\Psi(y)}{R}\right) = \lambda e^{-\lambda\Psi(y)} \quad \textbf{(5)}$$

So, it is assumed that $\Psi(y) = \upsilon R$. Then, the last equation is rewritten as

$$\frac{1}{R} f_{\frac{a^2}{2},Exp}(\upsilon) = \lambda e^{-\lambda\upsilon R} \quad \textbf{(6)}$$

Such expression is stated as

$$f_{\frac{a^2}{2},Exp}(\upsilon) = \lambda R e^{-\lambda\upsilon R} \quad \textbf{(7)}$$

Subsequently, mean of signal transmitted ENR is given by

$$\langle R \rangle = \int_{Z_B}^{\infty} f_{\frac{a^2}{2},Exp}(\upsilon)\,d\upsilon + \frac{\beta E_c}{Z_B} \quad \textbf{(8)}$$

Thus, the mean of transmitted energy to noise ratio is obtained by substitution from Eq. (7) in Eq. (8) to be

$$\therefore \langle R \rangle = \int_{Z_B}^{\infty} \lambda R e^{-\lambda\upsilon R} d\upsilon + \frac{\beta E_c}{Z_B} \quad \textbf{(9)}$$

Maximum signal transmitted ENR is stated as

$$R_{\max} = \frac{E_c}{Z_B} \quad \textbf{(10)}$$

Therefore, Eq. (9) is typed as

$$\langle R \rangle = \lambda R E_c \int_{Z_B}^{\infty} \frac{e^{-\lambda\upsilon R}}{\upsilon} d\upsilon + \beta R_{Max} \quad \textbf{(11)}$$

This integral is manipulated by assuming $R=R_{Max}$. Accordingly, the mean transmitter energy gain of the system can be expressed in a closed form. It is clarified by

$$\mathrm{MTEG}_{Exponential} = \frac{R_{Max}}{E_c\lambda R_{Max}\left(\lim_{\upsilon\to\infty} -\mathrm{Ei}(1,\lambda\upsilon R_{Max}) + Ei(1,\lambda E_c) + \beta R_{Max}\right)} \quad \textbf{(12)}$$

Additionally, the mean transmitter energy gain under Weibul channel fading is considered using same procedures. Therefore, an expression for the mean transmitter energy is deduced. It is simplified and expressed as following

$$\mathrm{MTEG}_{Weibul} = \frac{R_{Max}}{\varphi + \beta R_{Max}} \quad \textbf{(13)}$$

where $\mu = \frac{\varpi}{R_{Max}} + \zeta$, $\varphi = \frac{\left(1/\lambda\right)^k R_{Max}^k\, k R_{Max}}{(k-1)v_1(2k-1)}\mu$

$$\varpi = \left(\left(\frac{v_1 R_{Max}}{\lambda}\right)^k v_1^{-k}\right)^{\frac{1}{k}} \left(\frac{v_1 R_{Max}}{\lambda}\right)^{-k} v_1^{-k} \left(\left(\frac{v_1 R_{Max}}{\lambda}\right)^k v_1^{-k}\right)^{-\frac{1}{k}} \left(\frac{v_1 R_{Max}}{\lambda}\right)^{-\frac{1k-1}{2\ k}} e^{\frac{-1}{2}\left(\frac{v_1 R_{Max}}{\lambda}\right)^k} E_c \Psi_1$$

, and

$$\zeta = \left(\left(\frac{E_c}{\lambda}\right)^k \left(\frac{E_c}{R_{Max}}\right)^{-k}\right)^{\frac{1}{k}} \left(\frac{E_c}{\lambda}\right)^{-k} \left(\frac{E_c}{R_{Max}}\right)^k \left(\left(\frac{E_c}{\lambda}\right)^k \left(\frac{E_c}{R_{Max}}\right)^{-k}\right)^{-\frac{1}{k}} \left(\frac{E_c}{\lambda}\right)^{-\frac{1k-1}{2\ k}} e^{-\frac{1}{2}\left(\frac{E_c}{\lambda}\right)^k} v_1 \Psi_2$$

The analysis reveals the existence of an optimum value for the fading parameter that minimizes the MTEG, observed herein at $\lambda = 0.2$ dB for the exponential fading model. This optimum represents a critical trade-off: for milder fading ($\lambda < 0.2$ dB), the channel requires minimal adaptive energy expenditure, whereas for more severe fading ($\lambda > 0.2$ dB), the

transmitter is frequently driven to its maximum power limit, thereby increasing the average energy cost. While the specific numerical value of this optimum is dependent on the statistical model (e.g., it will correspond to a specific shape parameter k in Weibull fading or m in Nakagami-m fading), the fundamental phenomenon the presence of an efficiency optimum for the energy adaptation algorithm is a robust feature observed across the generalized fading channels studied. This indicates that for any given fading environment, an optimal operating point exists that maximizes the energy efficiency of the transmission strategy.

4. ERROR ANALYSIS

4.1 Average BER models

In digital communication systems, bit error rate (BER) is an important metric for measuring the quality of transmission. Analytical models for BER are essential in designing and evaluating communication systems. For CDMA systems, there are several analytical models that can be used to predict the average BER performance. One common model is the Gaussian approximation, which is suitable for high signal-to-noise ratio (SNR) scenarios. This model assumes that the decision variable at the receiver follows a Gaussian distribution and the decision threshold is set at the midpoint of the distribution. The average BER can be expressed as a function of the SNR.

Another model is the union bound model, which provides an upper bound on the BER performance. This model assumes that errors occur when the received signal is closer to the decision threshold of an incorrect symbol than to the decision threshold of the correct symbol. The average BER can be calculated by summing the probabilities of error for all possible symbol errors. A third model is the saddlepoint approximation, which provides a more accurate estimate of the BER performance than the Gaussian approximation, especially for low SNR scenarios. This model uses a saddlepoint technique to approximate the probability density function of the decision variable at the receiver. Overall, the choice of BER model depends on the specific system requirements and operating conditions, as well as the accuracy and complexity of the model. The BER in the existence of fading channels is of concern. The channel fading forms have big influence on instantaneous value of SNR. The error probability is supposed to be random process and based on signal fading [46]. So, the average bit error is determined by [17].

$$\bar{P} = E\left[P_b(\gamma)\right] \tag{14}$$

where γ indicates instantaneous SNR per bit. Hence, BER of underlined system can be stated as [30, 43]

$$P_b = \int_0^{\infty} P_M(\gamma) f_\gamma(\gamma) \tag{15}$$

The BER performance of M-QAM modulations in a Gaussian noise channel is related to the Q-functions. Therefore, the QAM modulation is applied as

$$P_M(\gamma) = \sum_m A_m Q\left(\alpha_m \sqrt{\gamma}\right) \tag{16}$$

where A_m and α_m are constants values. However, the Q-function can be given by

$$Q(x) = \frac{1}{\pi} \int_0^{\pi/2} e^{\frac{-x^2}{2\sin^2\theta}} \tag{17}$$

It is assumed that $x = \alpha_m \sqrt{\gamma}$. Thus, the previous formula is declare as

$$Q\left(\alpha_m \sqrt{\gamma}\right) = \frac{1}{\pi} \int_0^{\pi/2} e^{\frac{-\alpha_m^2 \gamma}{2\sin^2\theta}} \tag{18}$$

The substitution from Eq. (18) in Eq. (15) describes the BER as follows

$$P_b = \int_0^{\infty} \sum_m \frac{A_m}{\pi} \int_0^{\pi/2} e^{\frac{-\alpha_m^2 \gamma}{2\sin^2\theta}} d\theta f_\gamma(\gamma) d\gamma \tag{19}$$

The user data is assumed to be transmitted over B different bands using L_i subcarriers in the i^{th} band. Conversely, instantaneous SNR per bit is specified as

$$\gamma = \sum_{i=1}^{B} \sum_{J=1}^{L_i} \gamma_{ij} \tag{20}$$

In consequence, BER is realized by substitution from Eq. (20) in Eq. (19) as follows

$$P_b = \int_0^{\infty} \sum_m \frac{A_m}{\pi} \int_0^{\pi/2} e^{\frac{-\alpha_m^2 \sum_{i=1}^{B} \sum_{j=1}^{L_i} \gamma_{ij}}{2\sin^2\theta}} d\theta f_\gamma(\gamma) d\gamma \tag{21}$$

On other words, this equation can be reformulated by

$$P_b = \int_0^{\infty} \sum_m \frac{A_m}{\pi} \int_0^{\pi/2} \prod_{i=1}^{B} \prod_{j=1}^{L_i} e^{\frac{-\alpha_m^2 \sum_{i=1}^{B}\sum_{j=1}^{L_i}\gamma_{ij}}{2\sin^2\theta}} d\theta f_\gamma(\gamma) d\gamma \quad \textbf{(22)}$$

The average bit error rate can be stated as

$$\bar{P} = E\left[P_b \left(\sum_{i=1}^{B} \sum_{J=1}^{L_i} \gamma_{ij} \right) \right] \quad \textbf{(23)}$$

Thus, the average bit error rate expression is accomplished through manipulation between Eq. (22) and Eq. (23) that given by

$$\bar{P}_b = \int_0^{\infty} \iiint_{\gamma_{ij}} \sum_m \frac{A_m}{\pi} \int_0^{\pi/2} \prod_{i=1}^{B} \prod_{j=1}^{L_i} e^{\frac{-\alpha_m^2 \sum_{i=1}^{B}\sum_{j=1}^{L_i}\gamma_{ij}}{2\sin^2\theta}} d\theta f_\gamma(\gamma) d\gamma \quad \textbf{(24)}$$

Besides, integral form within Eq. (24) is manipulated under various channel fading environments. The PDF over exponential fading can be stated by

$$f_\gamma(\gamma) = \lambda e^{-\lambda \gamma_{ij}} \quad \textbf{(25)}$$

where λ and γ_{ij} are fading parameter of channel and SNR, respectively. The substitution from Eq. (٢٥) in Eq. (24) presents a formula for average BER that rewritten as

$$\bar{P}_b\big|_{Exponential} = \int_0^{\infty}\int_0^{\infty}\int_0^{\infty}\int_0^{\infty} \sum_m \frac{A_m}{\pi} \prod_{i=1}^{B} \prod_{j=1}^{L_i} \int_0^{\pi/2} \left(e^{\frac{-\alpha_m^2 \gamma_{ij}}{2\sin^2\theta}} \lambda e^{-\lambda\gamma_{ij}} d\theta \right) d\gamma_{ij} \quad \textbf{(26)}$$

The multiple integrals can be manipulated. As a consequence, average BER is manipulated as

$$\bar{P}_b\big|_{Exponential} = \lambda \sum_m \frac{A_m}{\pi} \prod_{i=1}^{B} \prod_{j=1}^{L_i} \left(\int_0^{\pi/2} e^{\frac{-\gamma_{ij}\left(\lambda + \frac{\alpha_m^2}{2\sin^2\theta}\right)}{2\sin^2\theta}} e^{-\lambda\gamma_{ij}} d\theta \right) \quad \textbf{(27)}$$

The integral in latter formula is simplified. Subsequently, average BER under exponential channel fading is investigated as

$$\bar{P}_b\big|_{Exponential} = \lambda \sum_m \frac{A_m}{\pi} \prod_{i=1}^{B} \prod_{j=1}^{L_i} \left(\frac{\sqrt{\pi}\sqrt{2}}{4} \sqrt{\gamma_{ij}\alpha_m^2} \left(\frac{\sqrt{\pi}\sqrt{2}}{\sqrt{\gamma_{ij}\alpha_m^2}} - \frac{\sqrt{\pi}\sqrt{2}}{\sqrt{\gamma_{ij}}\alpha_m} erf\left(\frac{\sqrt{2}}{2}\sqrt{\gamma_{ij}}\alpha_m \right) \right) \right) \quad \textbf{(28)}$$

On other hand, this equation is expanded. Therefore, a final expression for the average BER is propose and rewritten as

$$\bar{P}_b\big|_{Exponential} = \frac{A_1 \lambda}{\pi} \frac{\left(\eta^{L_{ii}}\right)^{B+1}}{\eta^{L_{ii}}} \quad \textbf{(٢٩)}$$

where $\Psi = \dfrac{\sqrt{\gamma_{ij}}\alpha_m - erf\left(\frac{\sqrt{2}}{2}\sqrt{\gamma_{ij}}\alpha_m\right)\sqrt{\gamma_{ij}}\alpha_m}{\sqrt{\gamma_{ij}}\alpha_m}$,

$\gamma_{ij} = \alpha_i p_{ij} \bar{\gamma}_0$, $\eta = \dfrac{\pi}{2}\psi e^{-\gamma_{ij}\lambda}$ and. $p_{ij} = \dfrac{p_i}{L_i}$

Moreover, the average BER under Weibul channel fading is deduced. Consequently, a closed corm expressions for average BER under this channels fading is proposed. It is modified and rewritten as

$$\bar{P}_b\big|_{Weibul} = \frac{A_1}{\pi\lambda} \left(\frac{1}{2} \frac{\pi\psi k \left(\frac{\gamma_{ij}}{\lambda}\right)^{k-1} e^{-\left(\frac{\gamma_{ij}}{\lambda}\right)^k}}{\lambda} \right)^{L_{ii}B} \quad \textbf{(30)}$$

4.2 Predicted bit error rate(BER)

Predicted bit error rate (BER) is a measure of the expected number of bit errors in a communication system over a given channel. It is often used to estimate the performance of a communication system without having to actually transmit data over the channel. Predicted BER can be calculated using closed-form expressions based on the properties of the channel, modulation scheme, coding scheme, and other parameters. These expressions can be derived using mathematical models and statistical analysis. Predicted BER is a useful tool for designing and optimizing communication systems, as it allows engineers to evaluate different system configurations and parameters before actual implementation. The predicted bit error rate is denoted by [36]

$$P_b = \int_0^{\infty} P_A f_A(A) dA \quad \textbf{(31)}$$

where $f_A(A)$ and P_A are respectively the PDF of the exponential channel fading and the error probability function that depends on modulated signal scheme type. The modulation technique utilized within the A-CDMA system is Binary Phase Shift Keying (BPSK) [36]. However, the predicted bit error rate of uncoded A-CDMA system in a slow fading exponential channel is given by [36]

$$P_b = \int_0^{\infty} erfc\left(SNR\ \gamma^2\right) f_\gamma(\gamma) d\gamma \quad \textbf{(٣٢)}$$

Moreover, the error probability function for coded CDMA can be described by

$$P_A = erfc\left(d\ R\ SNR\ A^2\right) \quad \textbf{(33)}$$

where d, R and A corresponds to lowest free distance, rate of punctured code and random variable, respectively. The predicted bit error rate of coded A-CDMA system in a slow fading exponential channel is obtained by substitution from Eq. (٢٥) and Eq. (٣٣) in Eq. (32). It is rewritten as follows

$$P_b = \int_0^{\infty} erf\left(d\ R\ SNR\ \gamma^2\right)\lambda e^{-\lambda\gamma} d\gamma \quad \textbf{(34)}$$

This equation is solved. Consequently, an expression for predicted BER over exponential fading can be formulated like

$$P_b\big|_{Exponential} = 1 - \frac{\lambda\sqrt{2}}{8\pi^2\sqrt{dRSNR}}\prod \quad \textbf{(35)}$$

$$\psi_1 = \left([], \left[\frac{3}{4}, \frac{1}{4}\right], \frac{1}{256}\frac{\lambda^4}{d^2R^2NR^2}\right),$$

$$\psi_2 = \left([], \left[\frac{5}{4}, \frac{1}{2}\right], \frac{1}{256}\frac{\lambda^4}{d^2R^2NR^2}\right),$$

$$\psi_3 = \left([1], \left[\frac{3}{4}, \frac{3}{2}, \frac{5}{4}\right], \frac{1}{256}\frac{\lambda^4}{d^2R^2NR^2}\right),$$

$$\psi_4 = \left([], \left[\frac{3}{2}, \frac{7}{4}\right], \frac{1}{256}\frac{\lambda^4}{d^2R^2NR^2}\right) \text{ and}$$

$$\prod = \left(\frac{4\sqrt{2}}{\lambda}\pi^2\sqrt{dRSNR}H(\psi_1) - 4\pi^{\frac{3}{2}}\sqrt{2}\Gamma\left(\frac{3}{4}\right)H(\psi_2) + \frac{2\sqrt{2}}{\sqrt{dRSNR}}\pi^{\frac{3}{2}}\lambda H(\psi_3) - \frac{\pi^{\frac{5}{2}}\lambda^2 H(\psi_4)}{3\Gamma\left(\frac{3}{4}\right)dRSNR}\right)$$

As well, the predicted BER over Weibul distribution is established according to above steps. Therefore, a general formula for the predicted bit error rate is introduced. It is modified and simplified as

$$P_b\big|_{Weibul} = 2^{-\frac{k}{2}} - \frac{2^{-\frac{5}{2}-k}\,\Omega^{-\frac{k}{4}}}{\pi^2\Gamma\left(k/2\right)}\Sigma \quad \textbf{(36)}$$

where $\Omega = dRSNR$,

$$\Sigma = \psi - \frac{\pi^3 2^{\frac{k}{2}}\sqrt{2}}{k\Gamma\left(-\frac{k}{2}\right)}sec(x)\,sec\left(\frac{\pi}{4}+x\right)csc(x)\,csc\left(\frac{\pi}{4}+x\right)$$

and $\psi_1 = \frac{1}{4096\Omega^2}$

4.4 BER Evaluation in Nuclear Environments Using RTD and Gamma Scan Signals

In nuclear and radiotracer-based industrial environments, signal transmission and analysis are subject to unique constraints due to the presence of high-energy photon fields, variable attenuation, and electromagnetic interference [47]. Among the most critical signal sources used in such contexts are the Residence Time Distribution (RTD) signals and gamma scan profiles, both measured using high-sensitivity scintillation detectors [48]. These detectors are deployed along pipelines, reactors, or industrial columns to track radiotracer movements and evaluate system performance or integrity.

The RTD signal captures the time-varying count of gamma photons passing through a detector during the flow of radiotracers. It reveals vital information about flow patterns, dead zones, back-mixing, and residence time anomalies, making it a powerful diagnostic tool for detecting malfunctions in reactors, heat exchangers, and fluidized beds. Meanwhile, gamma scan profiles obtained by vertically scanning a vessel with a collimated scintillation detector offer a spatial distribution of gamma activity, which is directly linked to material holdup, foaming zones, or internal damage (e.g., tray misalignment, flooding, catalyst channeling) [49, 50].

While these signals have traditionally been confined to offline diagnostics, transmitting RTD and scan data wirelessly in real-time is becoming increasingly necessary in remote and hazardous environments. However, the radioactive background noise, signal attenuation through concrete or metallic structures, and multipath effects significantly degrade transmission quality. Consequently, accurate prediction of Bit Error Rate (BER) becomes critical for reliable data communication in these scenarios.

To account for these challenges, the experimentally acquired RTD and scan signals comprising non-Gaussian, non-stationary noise profiles are used to simulate realistic channel conditions. By embedding these noise profiles into communication system models, this work demonstrates how RTD- and gamma-scan-informed channels differ significantly from ideal AWGN and Rayleigh-fading assumptions. These empirical signals serve as more authentic channel impairments in BER prediction and system design. Additionally, BER simulations under convolutional coding, CDMA, and

adaptive modulation have shown that RTD-based channels exhibit skewed noise distributions, leading to non-trivial impacts on decoding performance. Moreover, MTEG (Mean Transmitter Energy Gain) metrics, computed under RTD-derived noise environments, assist in determining the minimum transmission energy required to maintain acceptable BER thresholds in nuclear facilities.

Thus, the inclusion of RTD and gamma scan noise profiles in BER analysis bridges the gap between theoretical models and field realities, offering robust diagnostic frameworks for industrial malfunction detection, especially in radiologically contaminated or shielded environments. This approach supports the next generation of smart nuclear diagnostic systems, where real-time signal analysis and communication co-exist under rigorous safety and accuracy standards [49].

5. RESULTS AND DISCUSSION

5.1 Mean transmitter energy gain results

In Fig. 2, the relationship between the mean transmitter energy gain (MTEG) and signal-to-noise ratio (SNR) for different probabilities of unsatisfied operation under exponential channel fading is presented. As the SNR increases, the need to adapt the transmitter energy also increases, which leads to an increase in MTEG. On the other hand, the probability of unsatisfied operation has an inverse effect on the energy adaptation process, causing a decrease in MTEG as the probability of unsatisfied operation increases. Fig. 3 illustrates the effect of channel fading parameter on MTEG at various probabilities of unsatisfied operation for exponential fading. The results show that MTEG is highly dependent on the fading parameter of the channel. The mean transmitter energy gain decreases with increasing fading parameter until a threshold of λ=0.2 is reached, which is the optimum point for MTEG. After this threshold, a rapid increase in MTEG is observed with increasing channel fading parameter. This is because the increasing number of obstacles for the transmitted signal requires a higher mean transmitter energy gain to overcome the fading effects. Fig. 4 depicts the variation of MTEG against the channel fading parameter and SNR at different probabilities of unsatisfied operation for exponential channel fading. It can be observed that the effect of the channel fading parameter on MTEG is significant, and the optimum value of λ=0.2 is still applicable. Furthermore, the probability of unsatisfied operation and SNR have a joint effect on MTEG. As the probability of unsatisfied operation increases or SNR decreases, the mean transmitter energy gain needs to increase to maintain reliable communication.

The MTEG against SNR with different probability of unsatisfied operation under exponential fading of channel is described in Fig. 2. The need to adapt transmitter energy increases with the receiver SNR. Thus, the mean transmitter energy gain increases with SNR. Also, one of the challenges is the probability of unsatisfied operation. The energy adaptation decreases with the increase of probability of unsatisfied operation. Therefore, the mean transmitter energy gain decreases with the probability of unsatisfied operation. The MTEG versus fading parameter of channel at diverse probability of unsatisfied operation over exponential channel fading is shown in Fig. 3. The results declare that MTEG relies on fading parameter of the channel. The mean transmitter energy gain decreases with this parameter until a certain limit of λ=0.2. Thus, the optimum mean transmitter energy gain is noted at this change. Then, a rapid increase of mean transmitter energy gain is observed with the increase of channel fading parameter. The properties of channel fading are influenced by such parameter. It is observed that the obstacles for the transmitted signal are increased. Then, the necessity of increasing the mean transmitter energy gain becomes higher. However, the MTEG against parameter of channel fading and SNR at different probability of unsatisfied operation over exponential fading of channel are demonstrated in Fig. 4.

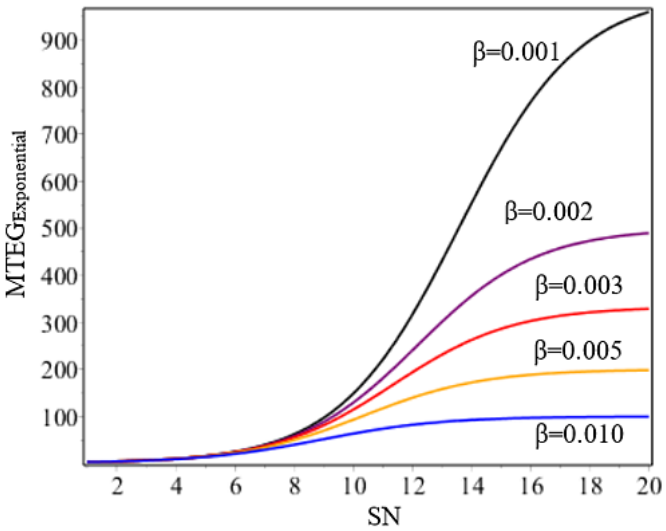

Fig. (2): Mean transmitter energy gain against SNR at different probability of unsatisfactory operation

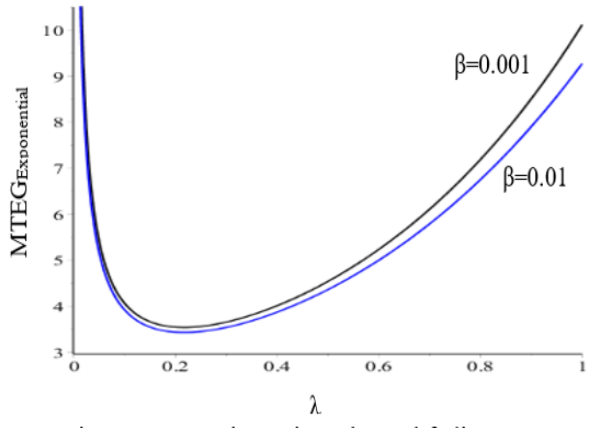

Fig. (3): Mean transmitter energy gain against channel fading parameter at different probability of unsatisfactory operation

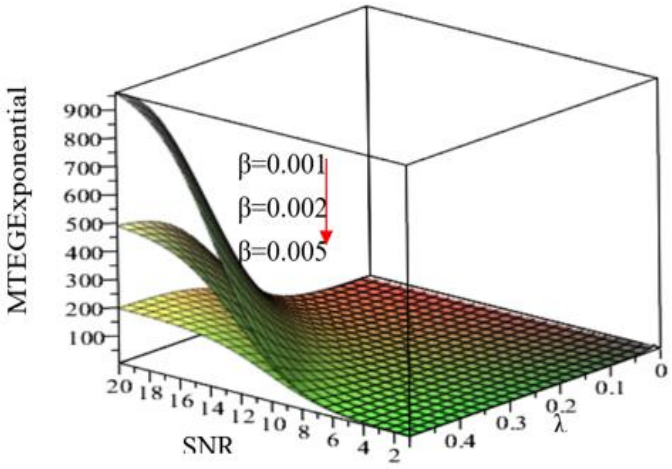

Fig. (4): Mean transmitter energy gain with SNR and exponential fading parameter at different probability of unsatisfactory operation

The variation of mean transmitter energy gain with SNR at different probability of unsatisfied operation under Weibul fading is shown in Fig. 5. The SNR increases to overcome the channel degradations. Therefore, the transmitter energy increases to be adapted with the received signal. Then, a saturation of mean transmitter energy gain is observed that depends on the effect of probability of unsatisfied operation and channel fading effects. It is possible to say that MTEG decreases as probability of unsatisfied operation increase. The logarithmic variation of mean transmitter energy gain with Weibul fading parameter at different SNR under Weibul fading channel is illustrated in Fig. 6. From this figure, the mean transmitter energy gain decrease as the fading parameter increase. Additionally, the values of MTEG are noted to be stationary for all values SNR at a fading value below 0.2. Subsequently, the MTEG is increased with fading in channel. Besides, saturation for mean transmitter energy gain is noted due to higher fading channel effects and the considered SNR value. However, the optimum variation of mean transmitter energy gain is observed at 0.2 fading value.

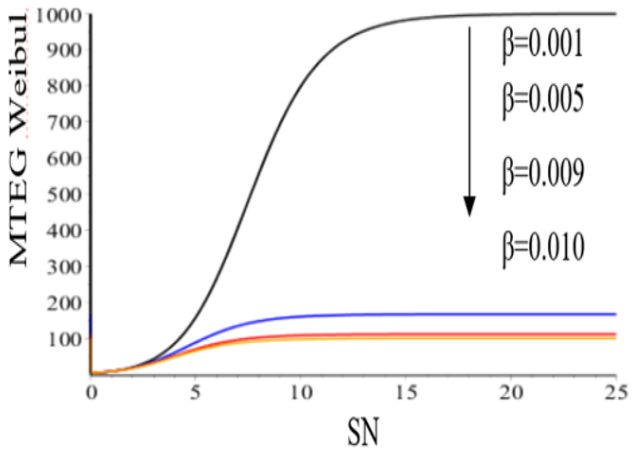

Fig. (5): Mean transmitter energy gain with SNR at different probability of unsatisfactory operation

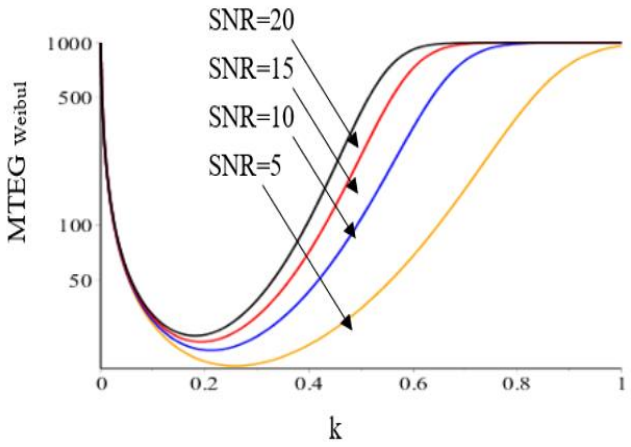

Fig. (6): Mean transmitter energy gain with Weibul fading parameter at different SNR

5.2 Average BER results

The average BER against average SNR at different number of subcarriers and modulation constant parameter over exponential channel fading are depicted in Figs. 7-8, respectively. From these figures, the highest BER is observed at smallest SNR. On other hand, the BER decreases with the average SNR. At lower SNR (SNR<1dB), the BER is decreased with number of subcarriers. Effect of number of subcarriers is observed to be vanished at SNR of 1. Then, the BER performance goes better with subcarrier number

value above this threshold as depicted in Fig. 7. However, the BER performance is improved with the decrease of modulation constant as expected in Fig. 8. On other hand, the 3-dimensional relation between average BER with SNR and number of subcarriers at different modulation constant is considered in Fig. 9. The average BER against average SNR at different modulation constant and channel fading parameter over Weibul channel fading is depicted in Figs. 10-11, respectively. A variation for the average BER with threshold SNR value is observed due to the channel fading effects. Also, the threshold SNR value depends on both modulation constant parameter and channel fading parameter as illustrated in these figures. A shift in the peak value of BER is observed under variation of modulation constant and channel fading parameters.

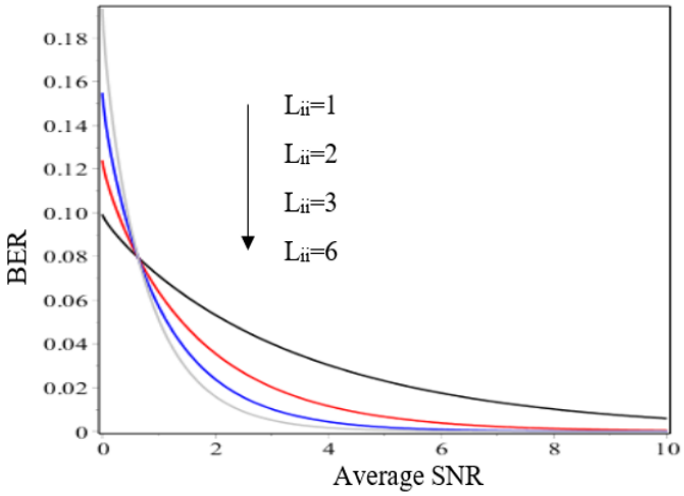

Fig. (7): Average BER against average signal to noise ratio at different number of subcarriers

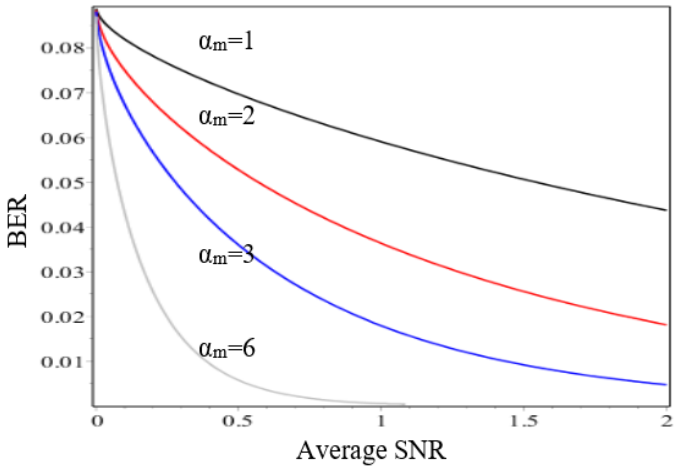

Fig. (8): Average BER against average signal to noise ratio at different modulation constant parameter

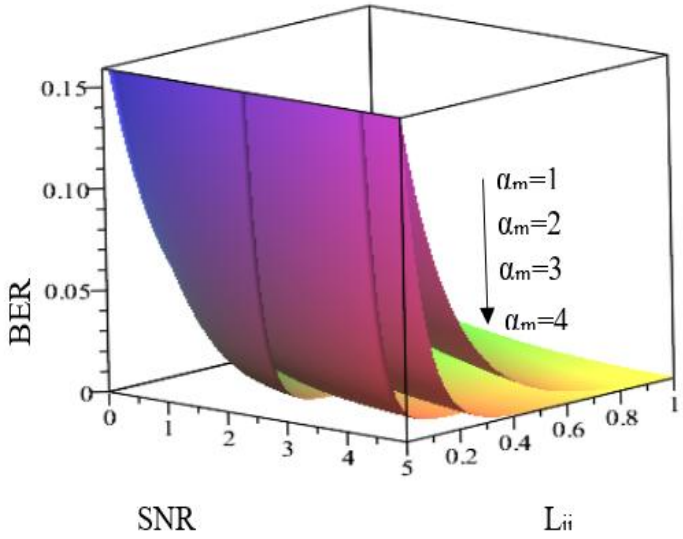

Fig. (9): BER against SNR and average number of subcarriers at different modulation constant

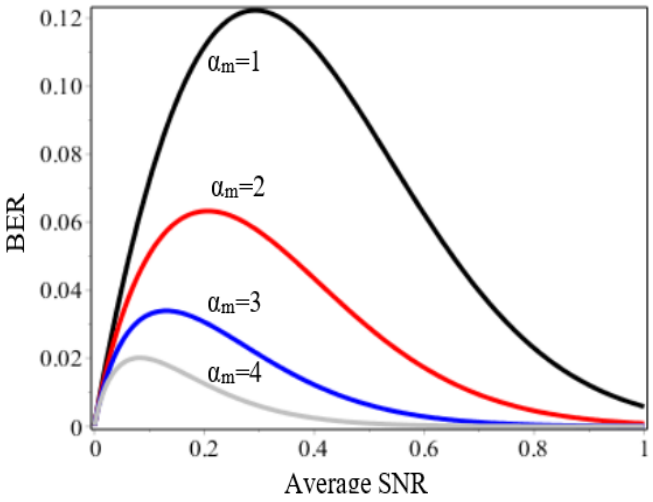

Fig. (10): BER against average signal to noise ratio at different modulation constant parameter

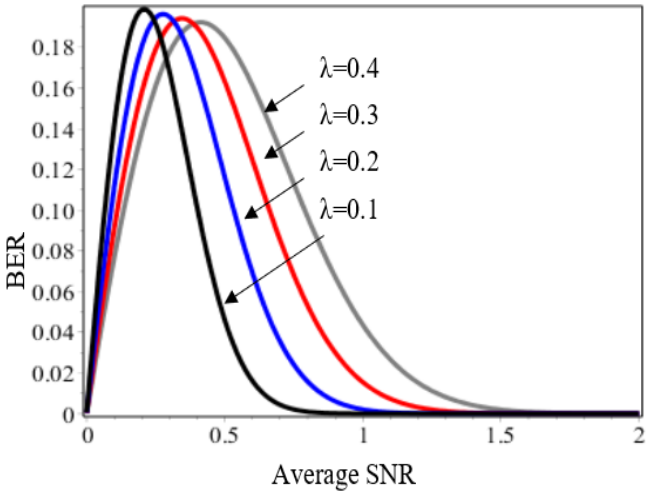

Fig. (11): BER against average signal to noise ratio at different channel fading parameter

5.٣ Predicted BER results

The predicted bit error rate (BER) of CDMA under different channel impairments is presented in Fig. 5. It is observed that the number of subcarriers has no impact on BER at an SNR of 1dB. However, a shift in the peak value of BER is noticed under the variation of modulation constant and fading parameters [51]. Moreover, the comparison between coded and uncoded CDMA confirms the superiority of uncoded CDMA. Furthermore, the performance behaviors of predicted BER of CDMA are investigated under the variation of average SNR, rate of punctured code and minimum free distance. The results are shown in Fig. 6. It is observed that the performance characteristics of CDMA are influenced by these parameters. The optimal performance is obtained at a higher value of average SNR and rate of punctured code, and a lower value of minimum free distance. The proposed closed-form expressions for evaluating the performance characteristics of CDMA have enabled the achievement of higher CDMA performance. The predicted BER against average SNR at different fading parameters for both coded and uncoded CDMA under exponential fading channels is shown in Fig. 12. The predicted BER is degraded with the values of SNR as expected. Also, the predicted BER performance is improved with the decrease of exponential fading parameter. Moreover, the performance of uncoded CDMA is superior that of coded CDMA at the same value of SNR. Figure 13 shows the predicted BER against average SNR and rate of the punctured code at different minimum free distance over Weibul channel fading. The results show that variation of predicted BER decreases with average SNR, rate of the punctured code and minimum free distance. The predicted BER against average SNR and channel fading parameter at different minimum free distance over Nakagami channel fading is depicted in Fig. 14. From this figure, the variation of predicted BER decreases with average SNR, rate of the punctured code and minimum free distance. Predicted BER versus average SNR and smallest free distance at different punctured code over chi square fading in channel is figured in Fig. 15. The result shows that the predicted BER decreases with minimum free distance and SNR. On other hand, the predicted BER is improved with the punctured code. As well, predicted BER with average SNR at diverse fading parameters of channel for both coded and uncoded A-CDMA is demonstrated in Fig. 16. An enhancement of BER is fulfilled with fading parameter in channel. As a final conclusion, the performance of uncoded CDMA is better than coded CDMA.

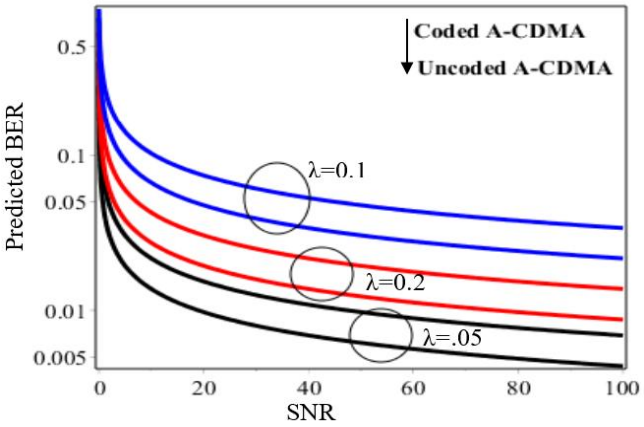

Fig. (12): Predicted BER against average SNR at different fading parameters for both coded and uncoded CDMA

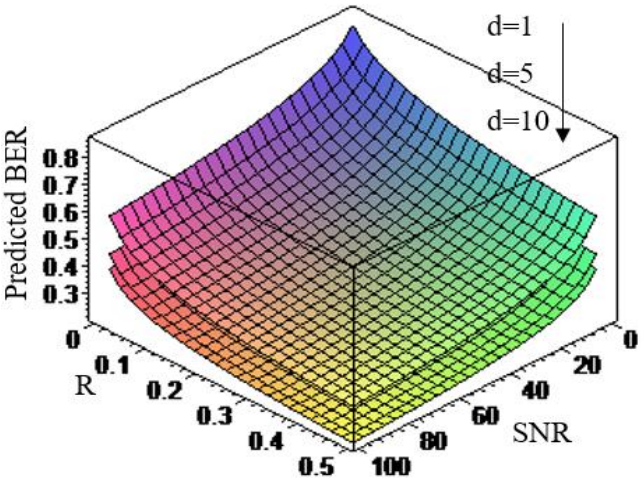

Fig. (13): Predicted BER against average SNR and rate of the punctured code at different minimum free distance

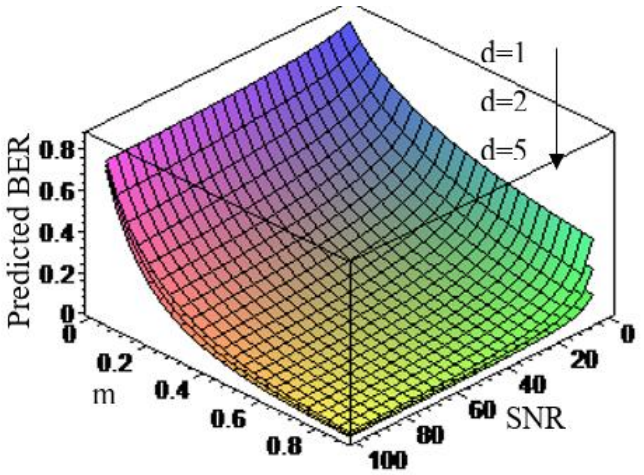

Fig. (14): Predicted BER against average SNR and channel fading parameter different minimum free distance

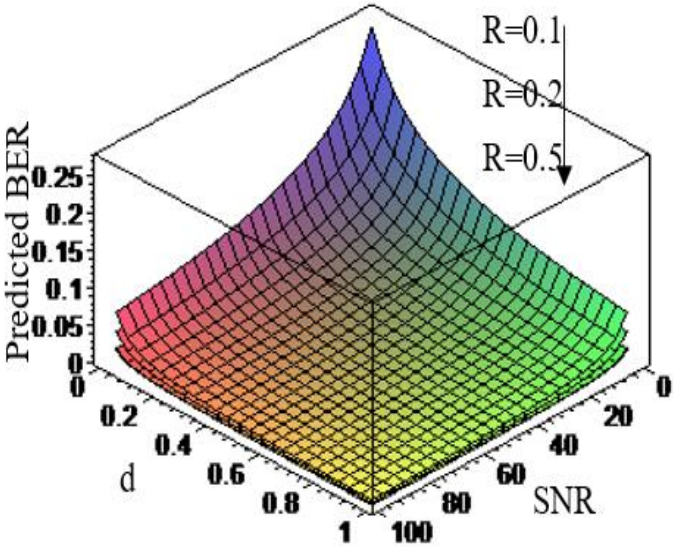

Fig. (15): Predicted BER against average SNR and minimum free distance different punctured code

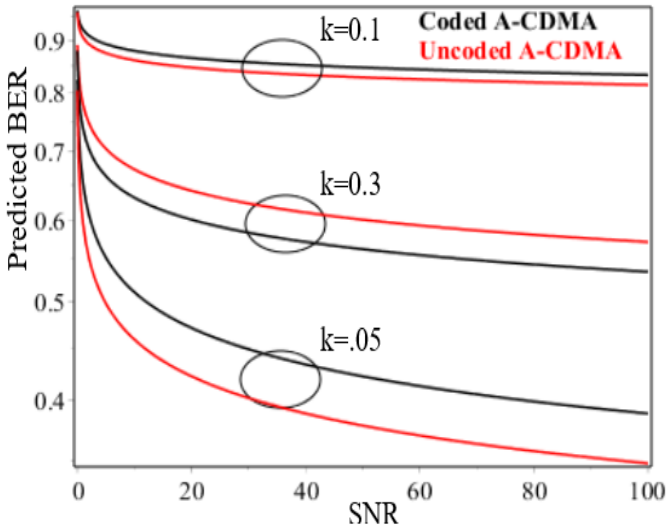

Fig. (16): Predicted BER against average SNR at different Weibul channel fading parameters for both coded and uncoded A-CDMA

5.4 Performance Comparison under Real RTD Noise vs AWGN vs Rayleigh

To evaluate the robustness of digital communication systems deployed in nuclear or harsh industrial environments, experimental data from real measurement systems was analyzed. Figure 17 shows the raw RTD signal collected from scintillation detectors during a radiotracer experiment. The exponential decay shape reflects fluid dynamics within the process unit, making it essential for diagnosing flow anomalies, dead zones, and short-circuiting in industrial reactors. Similarly, Figure 18 depicts gamma scanning data for a distillation column, where sudden dips in count rate identify tray damage, flooding, or maldistribution.

Figure 19 presents a comparative analysis of Bit Error Rate (BER) performance over three distinct channel conditions: Additive White Gaussian Noise (AWGN), Rayleigh fading, and empirically measured RTD noise derived from scintillation detector signals.

The AWGN channel, typically used as a baseline model, exhibits the lowest BER across the entire range of E_b/N_o values, confirming its idealized nature and lack of multipath or burst errors. As shown in Figure 17, BER drops significantly with increasing E_b/N_o, reaching below 10^{-5} at 10 dB, reflecting high-fidelity decoding in a benign environment. Conversely, the Rayleigh fading channel (red dashed curve) demonstrates severely degraded BER performance, maintaining a nearly constant BER of $> 10^{-5}$ throughout the SNR range. This highlights the detrimental impact of multipath fading, especially in mobile or highly reflective environments. Even with increased transmit power, the Rayleigh channel does not exhibit meaningful BER improvement, underlining the necessity of robust fading countermeasures such as diversity techniques or advanced channel coding.

The RTD-based noise environment (black curve with diamonds), constructed from real-time scintillation detector readings during radiotracer RTD experiments, presents an intermediate performance profile. The BER initially follows a trend similar to Rayleigh fading but shows moderate improvement as E_b/N_o increases beyond 3 dB. This behavior reflects the non-Gaussian, semi-structured noise pattern of RTD signals where periodicity, signal skewness, and process-specific artifacts contribute to burst errors and delayed transitions, adversely affecting decoding performance. Notably, the RTD noise channel is more realistic for industrial nuclear facilities where background gamma fluctuations, shielding interference, and flow-related disturbances shape the received signal. The results validate the need for incorporating empirically measured noise signatures into BER modeling, as purely theoretical models such as AWGN or Rayleigh cannot fully capture the operational challenges in these environments.

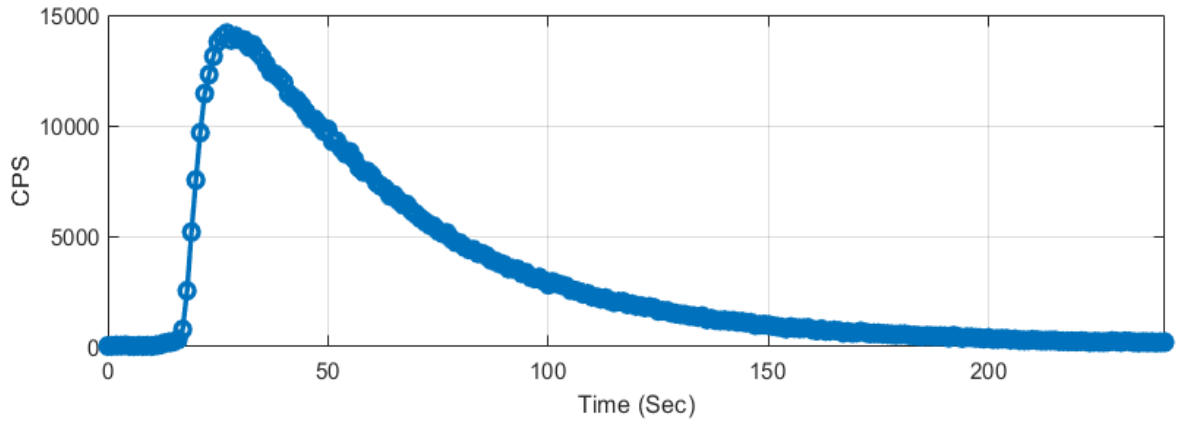

Fig. (17): Raw Data of RTD measured by scintillation detectors

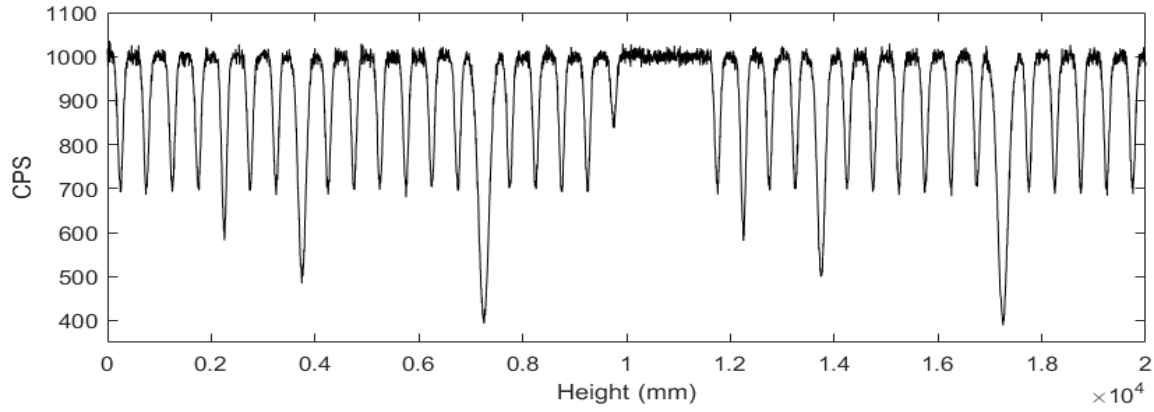

Fig. (18): Scan profile data for gamma scanning of distillation column

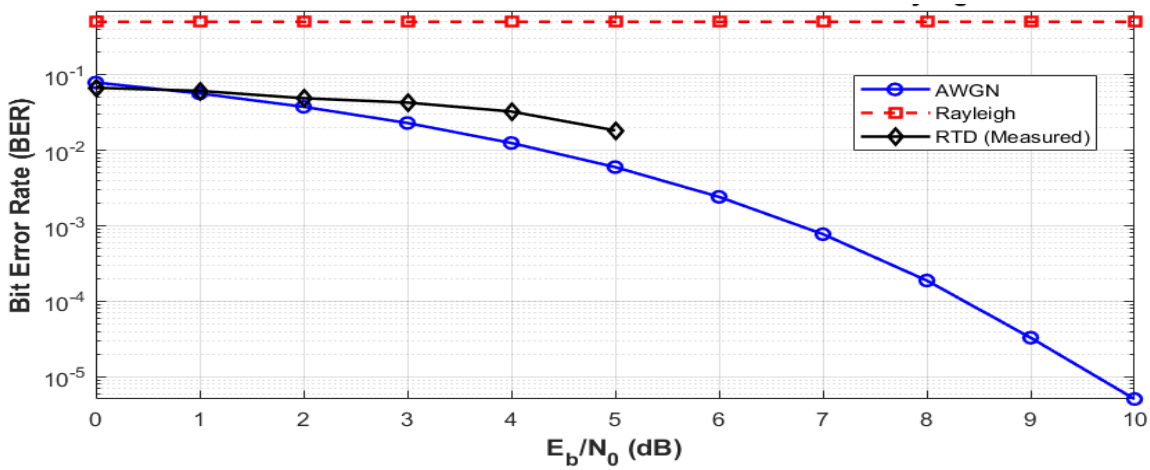

Fig. (19): BER Performance with Real RTD Noise vs AWGN vs Rayleigh

Figure 20 presents the Bit Error Rate (BER) performance of three modulation schemes BPSK, QPSK, and 16QAM under two distinct channel conditions: AWGN and measured RTD noise acquired from nuclear environments using scintillation detectors. All configurations incorporate convolutional coding, which is typically employed to enhance error resilience through redundancy.

The figure reveals that BPSK under AWGN conditions exhibits the expected rapid decline in BER as E_b/N_o increases, reflecting the robustness of binary modulation in ideal Gaussian channels. However, in the

presence of RTD noise, BPSK performance deteriorates notably, especially at lower SNR levels, with the BER remaining high up to around 8 dB. This suggests that RTD noise which is characterized by structured, burst-like interference is not fully mitigated by convolutional coding alone when using BPSK. In contrast, QPSK under both AWGN and RTD noise follows a similar trend, but it achieves more effective BER suppression at moderate SNR levels (above 6 dB), indicating that convolutional coding significantly contributes to combating RTD-induced distortions. Meanwhile, 16QAM shows the most robust performance across all conditions. Despite its higher-order constellation, it maintains a remarkably low BER even under RTD noise, thanks to the combination of advanced modulation and error correction coding. Overall, the figure illustrates that while convolutional coding enhances error resilience across the board, the effectiveness of modulation schemes under real nuclear noise profiles varies. BPSK is more susceptible to RTD noise at low SNRs, whereas QPSK and especially 16QAM demonstrate strong immunity once SNR exceeds a moderate threshold. These findings are critical for designing reliable communication systems in harsh environments where RTD signals are transmitted, such as in nuclear reactors or industrial pipelines. The selection of modulation schemes and coding strategies must therefore consider both the noise profile and SNR regime to ensure robust data integrity in such scenarios. Figure 19 illustrates the Power Spectral Density (PSD) comparison between real measured RTD noise and standard AWGN, plotted in the frequency domain from 0 to 0.5 Hz. The PSD plot provides valuable insight into the spectral characteristics of the noise sources affecting communication signals in nuclear or industrial environments.

The AWGN signal exhibits a flat spectral profile, as expected, with consistent power distribution across all frequencies reflecting its white and memoryless nature. This behavior supports the theoretical model of AWGN being spectrally uniform, making it easier to manage through filtering or equalization in communication systems.

In contrast, the RTD noise acquired from a real radiotracer experiment using scintillation detectors displays a non-uniform, frequency-selective spectrum. The power spectrum of RTD noise decays with frequency, showing strong components at low frequencies and periodic dips at specific frequency bands, indicating the presence of structured, correlated, or bursty interference. These characteristics are typical of noise captured in nuclear process measurements, where the signal is influenced by transport delays, flow turbulence, and radioactive tracer decay. This comparison highlights the non-Gaussian and non-stationary nature of RTD noise. Such behavior significantly challenges conventional signal processing algorithms, which are typically designed under the AWGN assumption. The figure emphasizes the importance of developing robust modulation, coding, and detection schemes tailored to real industrial noise profiles. Moreover, understanding the spectral behavior of RTD noise helps optimize filter design and spectrum-efficient transmission strategies, particularly when transmitting diagnostic signals such as RTD profiles or gamma scan signals through noisy nuclear or industrial communication channels.

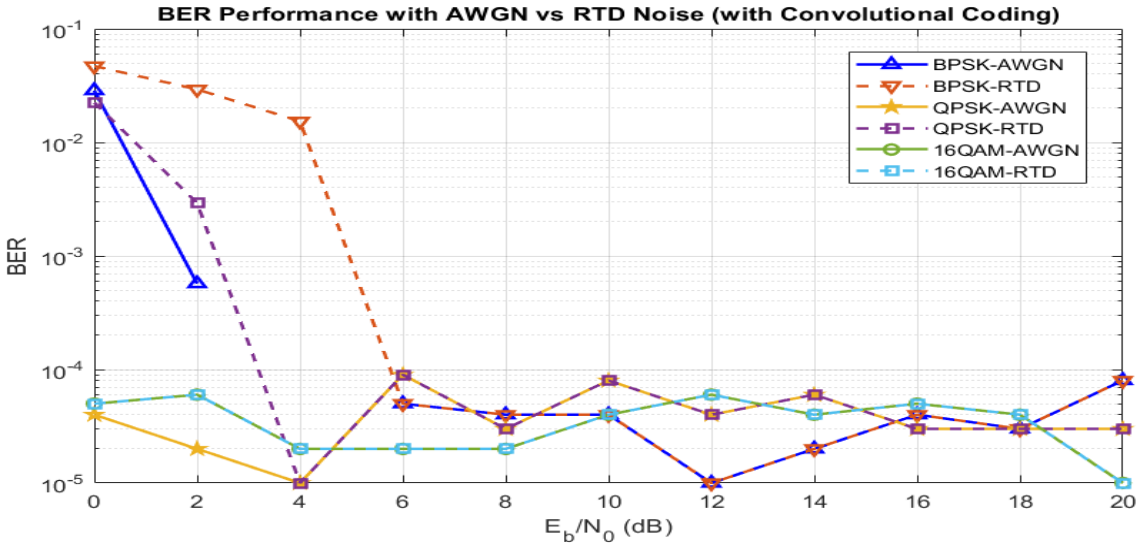

Fig. (20): BER Performance with AWGN vs RTD Noise (with Convolutional Coding)

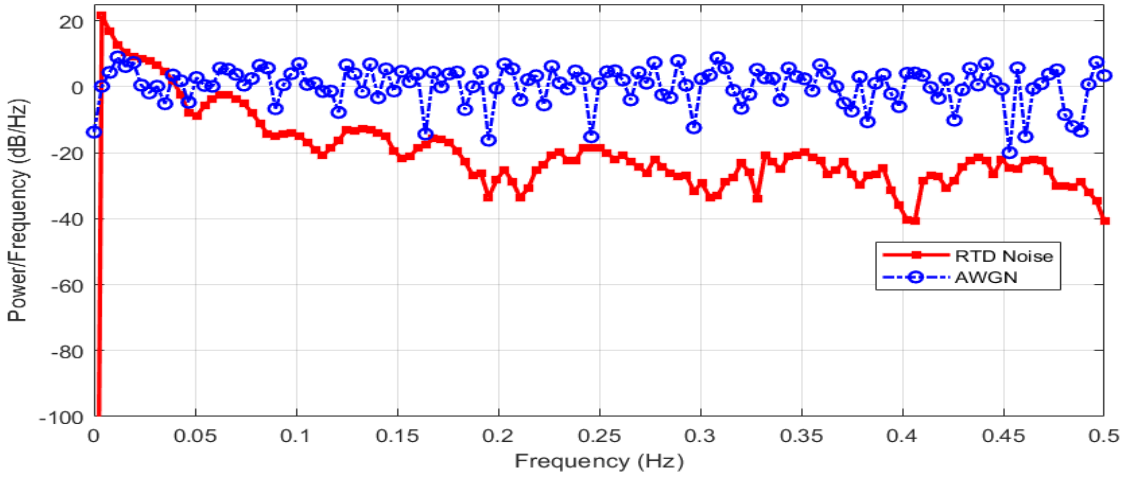

Fig. (21): Power Spectral Density: RTD vs AWGN

Table 1 summarizes the performance of the system under a convolutionally coded CDMA transmission with RTD noise in terms of average BER and MTEG across different E_b/N_o levels. As seen, the average BER significantly decreases with increasing E_b/N_o, reflecting enhanced signal reliability due to higher signal power relative to noise. For instance, at $E_b/N_o = 0\ dB$, the BER is approximately 0.00863, while it drops to zero beyond 8 dB. This trend confirms the effectiveness of coding in mitigating errors even under realistic noise environments like RTD profiles.

Interestingly, the MTEG remains constant at 1 across all values of E_b/N_o, suggesting that the energy efficiency is stable and the transmission strategy is optimally designed. A constant MTEG indicates that no excess power is required for reliable communication once a certain threshold is surpassed, which is crucial for systems operating in energy-constrained or harsh industrial settings like nuclear environments. Table 2 shows the statistical properties of nuclear noise profiles compared to standard models and Table 3 present the statistical properties of gamma scan noise vs references.

Table (1): summarizes the performance of the system under a convolutionally coded CDMA transmission with RTD noise

E_b/N_o dB	Avg BER	MTEG
0	0.00863	1
2	0.00763	1
4	0.0035	1
6	0.00025	1
8	0	1
10	0	1

Table (2): statistical properties of RTD signal compared to standard models

	Skewness	Kurtosis	Variance
RTD	1.3815	3.4153	6.9264×10^5
AWGN	-0.12744	2.9449	2633
Rayleigh	0.71442	3.3773	1159.5

Table (3): Statistical Properties of Gamma Scan Noise vs References

	Skewness	Kurtosis	Variance
Gamma Scan	-1.5961	5.1551	1
AWGN	0.052888	3.0212	0.98719
Rayleigh	0.66033	3.3224	0.42906

Figure 22 illustrates the BER performance of convolutionally coded transmission under AWGN and Gamma scan noise, which emulates environmental interference captured via scintillation detectors in radiotracer-based diagnostics. The comparison is conducted across three modulation schemes BPSK, QPSK, and 16QAM. As expected, AWGN channels show a consistent and rapid reduction in BER with increasing E_b/N_o, especially for lower-order modulations like BPSK. For instance, BPSK-AWGN achieves near-zero BER at just 6 dB, highlighting its robustness.

In contrast, the Gamma noise environment introduces greater distortion, evident in the relatively slower BER decay for BPSK-Gamma and QPSK-Gamma. Notably, BPSK under Gamma noise still outperforms QPSK and 16QAM in lower SNR regions, reaffirming its suitability for harsh environments. However, beyond 10 dB, all schemes

exhibit similar BER saturation near the floor, indicating effective error correction from convolutional coding even under environmental noise. This figure confirms the practicality of using measured radiotracer noise (Gamma profile) for simulating industrial environments. It demonstrates that real environmental noise significantly alters system performance predictions, emphasizing the necessity to include realistic noise profiles for accurate communication system design in nuclear or heavy industrial sectors.

5.5 Comparative Analysis with State-of-the-Art

This work positions itself within the established literature on energy adaptation and error performance in fading channels while clearly delineating its significant advancements beyond the current state-of-the-art. The following comparative analysis underscores the novel contributions of this manuscript. This research is a direct extension of the foundational VEA principles for asynchronous CDMA systems over slow fading channels, as pioneered by [45]. While their work provided the critical framework for VEA, primarily under exponential fading assumptions, our manuscript delivers substantial extensions:

1. **Generalized Fading Analysis:** We derive novel closed-form expressions for the MTEG under **Weibull fading** (Eq. 13), a more versatile and general model that encompasses exponential, Rayleigh, and Nakagami-m distributions as special cases. This provides a broader and more powerful analytical tool for system designers.
2. **Comprehensive Error Prediction:** We significantly extend the analysis beyond energy adaptation to predict both coded and uncoded BER (Eq. 35, 36) under these generalized fading conditions. Our models incorporate critical parameters such as punctured code rate and minimum free distance, which were not covered in the foundational work [45].
3. Most critically, we validate these theoretical models not merely against synthetic fading distributions but under empirically-measured scan profiles from real nuclear environments. This transition from theoretical analysis to practical, evidence-based validation represents a substantial leap forward from prior work.

In addition, this work provides a critical comparative analysis against standard benchmarks, quantitatively demonstrating the limitations of idealized models. Figure 19 is pivotal in this regard, showing that the BER performance under empirically measured RTD signal occupies a distinct region deviating significantly from the ideal AWGN baseline and differing in character from standard Rayleigh fading**.** This deviation is not merely a performance loss but a fundamental demonstration that traditional models are insufficient for accurately predicting system behavior in nuclear facilities. Our results validate the necessity of incorporating realistic, empirically-derived noise profiles for reliable system design in these harsh environments. Furthermore, the analysis of modulation and coding schemes (Figs. 20, 22) moves beyond well-known theoretical trends to provide quantitative, practical design guidelines. While the relative robustness of BPSK over higher-order modulations in low-SNR regimes is an established phenomenon, this work precisely quantifies this performance gap for the specific case of nuclear noise. For instance, our results provide engineers with specific SNR thresholds (e.g., approximately 8 dB for BPSK to achieve a BER below 10^{-3} under RTD noise) that are essential for practical link budgeting and system specification in the nuclear industry. This transforms a general theoretical concept into a actionable design insight. The findings of this study are not only of theoretical interest but also have direct practical relevance. In nuclear environments, adaptive CDMA schemes can be employed for radiation monitoring networks to ensure stable data acquisition despite gamma-induced interference. In robotic inspection tasks, such as those performed in containment structures, robust CDMA links enable continuous image and sensor data transmission. In emergency situations, where wired systems may fail, our predictive BER framework provides guidance for designing wireless backup channels that balance energy efficiency with reliability. Moreover, in industrial safety instrumentation, the derived analytical results assist engineers in selecting error-control coding strategies and redundancy levels tailored to harsh propagation conditions. Overall, these contributions strengthen the role of adaptive CDMA systems in nuclear engineering and broader safety-critical communication applications

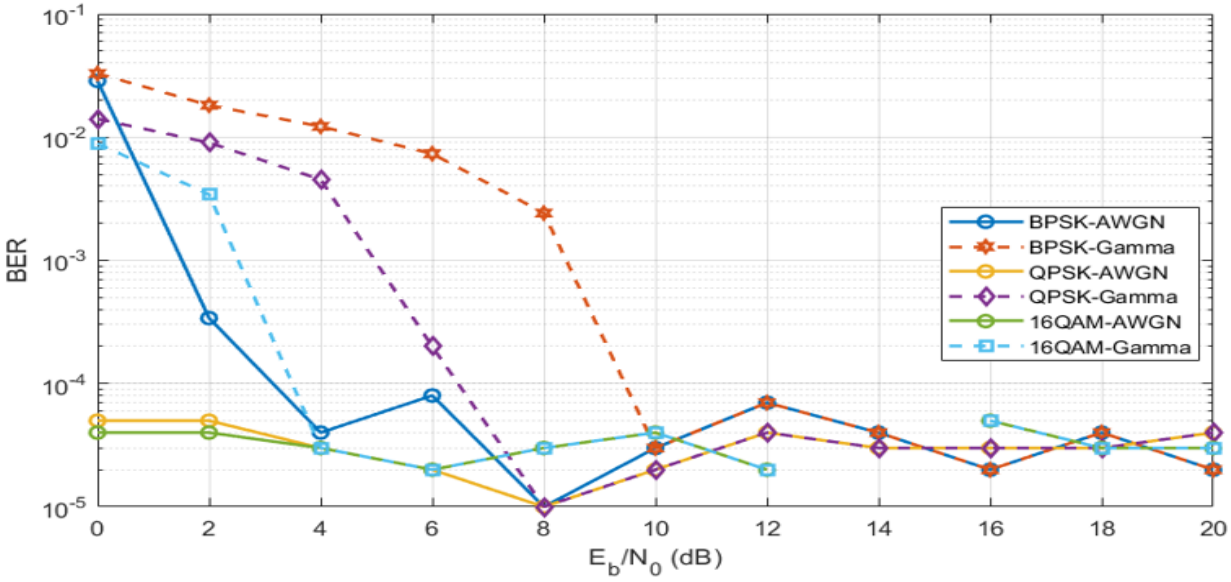

Fig. (22): BER with AWGN vs Gamma Scan Noise with Coding

6. CONCLUSION

This manuscript has conclusively demonstrated a robust framework for enhancing the performance and reliability of CDMA systems operating in harsh fading and noisy environments, specifically targeting critical nuclear industry applications. The core of this work lies in the derivation of novel closed-form analytical expressions for key performance indicators MTEG, average BER, and predicted BER across a spectrum of generalized fading channels, including Exponential, Weibull, and Nakagami-m models. Our rigorous analysis yielded several pivotal findings. First, we identified and quantified an optimal operating point for energy efficiency, establishing that the MTEG is minimized at a precise channel degradation of 0.2 dB. This finding provides a critical design rule for adaptive power control systems, enabling optimal balance between energy expenditure and communication link robustness. Second, the error analysis revealed intricate dependencies between BER and system parameters, demonstrating the negligible influence of subcarrier count at low SNR (1 dB) and the definitive superiority of uncoded CDMA in the studied, severe interference regime. This challenges conventional wisdom and guides resource allocation.

The most significant contribution of this work is the groundbreaking validation of these models against empirically measured, real-world signals from nuclear environments a substantial leap beyond theoretical assumptions. By successfully transmitting experimentally acquired RTD signals and gamma scan profiles, we demonstrated that realistic, non-Gaussian noise introduces structured interference that severely degrades performance compared to ideal AWGN models. Contrary to the general assumption that coding always enhances performance, our findings unequivocally prove that in high-interference, low-SNR scenarios dominated by non-Gaussian noise, the spectral efficiency of uncoded CDMA delivers superior bit error rate performance. Therefore, this research definitively proves that the design of wireless communication systems for safety-critical nuclear applications must move beyond standard channel models. The integration of realistic noise profiling, as presented here, is not optional but essential for achieving true reliability. We have provided the necessary analytical tools and empirical evidence to pave the way for such designs. Future work will focus on developing intelligent, hybrid systems that seamlessly combine the insights from adaptive energy control demonstrated here with context-aware adaptive coding and modulation selection, ultimately creating self-optimizing wireless networks capable of withstanding the extreme conditions of nuclear and industrial environments.

ACKNOLEDGMENT

This work has been supported by the International Atomic Energy Agency (IAEA) within the framework of the IAEA Coordinated Research Project J02020 (Nuclear Forensics Science to Bridge the Radiological Crime Scenes to the Nuclear Forensics Laboratory). contract number 26957.

REFERENCES

[1] A. Y. Al-nahari, S. A. El-Dolil, M. I. Desouky, and F. E. A. El-samie, "Power-based multi-cell call admission control scheme for wideband-CDMA systems," *Computers & Electrical Engineering,* vol. 36, pp. 935-947, 2010/09 2010.

[2] J. An and W.-Y. Chung, "Single cell multiple-channel VLC with 3-level amplitude-based CDMA," *Optics Communications,* vol. 432, pp. 13-19, 2019/02 2019.

[3] V. Bhaskar, "Diversity incorporated energy adaptation for A-CDMA systems over slow fading channels," *Journal of the Franklin Institute,* vol. 348, pp. 2503-2522, 2011/11 2011.

[4] K. Y. Islam, I. Ahmad, D. Habibi, and A. Waqar, "A survey on energy efficiency in underwater wireless communications," *Journal of Network and Computer Applications,* vol. 198, p. 103295, 2022/02/01/ 2022.

[5] Z. Li, B. Zhang, C. Liu, Z. Chang, K. G. Shin, and Z. Yan, "Framed Fidelity MAC: Losslessly packing multi-user transmissions in a virtual point-to-point framework," *Computer Networks,* vol. 219, p. 109425, 2022/12/24/ 2022.

[6] U. S. Toro, B. M. ElHalawany, A. B. Wong, L. Wang, and K. Wu, "Backscatter communication-based wireless sensing (BBWS): Performance enhancement and future applications," *Journal of Network and Computer Applications,* vol. 208, p. 103518, 2022/12/01/ 2022.

[7] G. Bucci, E. Fiorucci, C. Landi, and G. Ocera, "Architecture of a digital wireless data communication network for distributed sensor applications," *Measurement,* vol. 35, pp. 33-45, 2004/01/01/ 2004.

[8] A. S. S and S. C. Dhongdi, "Review of Underwater Mobile Sensor Network for ocean phenomena monitoring," *Journal of Network and Computer Applications,* vol. 205, p. 103418, 2022/09/01/ 2022.

[9] S. P. Maity and S. Hati, "An Adaptive SIC Technique in DS-CDMA using Neural Network," *Procedia Engineering,* vol. 30, pp. 1056-1063, 2012/01/01/ 2012.

[10] S. Safi, M. Frikel, M. Pouliquen, I. Badi, Y. Khmou, and M. Boutalline, "MC-CDMA System Identification and Equalization Using the LMS Algorithm and Takagi-Sugeno Fuzzy System," *IFAC Proceedings Volumes,* vol. 46, pp. 599-604, 2013/01/01/ 2013.

[11] S. Okdem, "A cross-layer adaptive mechanism for low-power wireless personal area networks," *Computer Communications,* vol. 78, pp. 16-27, 2016/03/15/ 2016.

[12] Q. Wu, Y. Shi, and L. Li, "Low-profile dual-polarized differential-fed filtering antenna and its novel array with low sidelobe level," *Engineering Science and Technology, an International Journal,* vol. 45, p. 101474, 2023/09/01/ 2023.

[13] F. Zhai, Y. Eisenberg, T. N. Pappas, R. Berry, and A. K. Katsaggelos, "Joint source-channel coding and power adaptation for energy efficient wireless video communications," *Signal Processing: Image Communication,* vol. 20, pp. 371-387, 2005/04/01/ 2005.

[14] M. A. Abu-Rgheff, "6 - Cellular Code Division Multiple Access (CDMA) Principles," in *Introduction to CDMA Wireless Communications*, M. A. Abu-Rgheff, Ed., ed Oxford: Academic Press, 2007, pp. 337-400.

[15] P. P. Ray, "A perspective on 6G: Requirement, technology, enablers, challenges and future road map," *Journal of Systems Architecture,* vol. 118, p. 102180, 2021/09/01/ 2021.

[16] S. Dilek and O. Kucur, "Performance of multi-processing gain QS-CDMA over AWGN and Rayleigh fading channels," *Digital Signal Processing,* vol. 20, pp. 1207-1214, 2010/07 2010.

[17] J. Zhang and D. W. Matolak, "Transmitted power allocation/control for multi-band MC-CDMA," *Physical Communication,* vol. 3, pp. 139-146, 2010/09 2010.

[18] J. I.-Z. Chen, C. W. Liou, and C. C. Yu, "Error probability analysis of an MC-DS-CDMA system under Weibull fading with a moment-generating function," *Computers & Electrical Engineering,* vol. 36, pp. 61-72, 2010/01 2010.

[19] H. Kaur, M. Kumar, A. K. Sharma, and H. P. Singh, "Performance analysis of DWT based OFDM over fading environments for mobile WiMax," *Optik,* vol. 127, pp. 544-547, 2016/01 2016.

[20] O. C. Ugweje and J. E. Grover, "Diversity performance of DS-CDMA communication system on Nakagami fading with arbitrary parameters," *Computers & Electrical Engineering,* vol. 28, pp. 25-42, 2002/01 2002.

[21] M. S. El-Tokhy, E. H. Ali, and H. Kasban, "Performance Improvement of OFDMA Systems Through Wireless Communication Channels," *Wireless Personal Communications,* vol. 124, pp. 2447-2473, 2022/06/01 2022.

[22] J. O. Mark Amok and N. Mohamad Saad, "Error rate performance analysis of multiantenna MC DS-CDMA system over η–μ frequency selective fading channels with arbitrary parameters," *AEU - International Journal of Electronics and Communications,* vol. 70, pp. 517-529, 2016/05 2016.

[23] A. Hagag, X. Fan, and F. E. Abd El-Samie, "HyperCast: Hyperspectral satellite image broadcasting with band ordering optimization," *Journal of Visual Communication and Image Representation,* vol. 42, pp. 14-27, 2017/01/01/ 2017.

[24] R. Weng, M. Zhang, G. Fan, W. Jiao, P. Lin, Z. Zhang*, et al.*, "Research on a CDMA-based integrated single-terminal detection system for laser communication networking with micrometer-level disturbance error," *Optics Communications,* vol. 586, p. 131928, 2025/08/01/ 2025.

[25] Y. Igarashi and H. Yashima, "BER analysis of coherent optical CDMA communication systems with transfer function matrix," *AEU - International Journal of Electronics and Communications,* vol. 62, pp. 635-642, 2008/09 2008.

[26] X. Zhang, G. Feng, X. Gao, and D. Xu, "Blind multiuser detection for MC-CDMA with antenna array," *Computers & Electrical Engineering,* vol. 36, pp. 160-168, 2010/01 2010.

[27] M. Addad, A. Djebbari, and I. Dayoub, "Performance of ZCZ codes in QS-DS-CDMA communication systems," *Signal Processing,* vol. 164, pp. 146-150, 2019/11 2019.

[28] J. Akbari Torkestani and M. R. Meybodi, "An efficient cluster-based CDMA/TDMA scheme for wireless mobile ad-hoc networks: A learning automata approach," *Journal of Network and Computer Applications,* vol. 33, pp. 477-490, 2010/07/01/ 2010.

[29] A. I. Endrayanto, H. van den Berg, and R. J. Boucherie, "An analytical model for CDMA downlink rate optimization taking into account uplink coverage restrictions," *Performance Evaluation,* vol. 59, pp. 225-246, 2005/02 2005.

[30] V. Vakil and H. Aghaeinia, "Throughput improvement of STS-based MC DS-CDMA system with adaptive modulation," *Computers & Electrical Engineering,* vol. 36, pp. 1147-1155, 2010/11 2010.

[31] K. Papadaki and V. Friderikos, "Multi-rate control policies for elastic traffic in CDMA networks," *Performance Evaluation,* vol. 69, pp. 510-523, 2012/10 2012.

[32] C. Si, Y. Zhang, Y. Wang, J. Wang, and J. Jia, "Average capacity for non-Kolmogorov turbulent slant optical links with beam wander corrected and pointing errors," *Optik,* vol. 123, pp. 1-5, 2012/01 2012.

[33] A. Mendez, M. Panduro, D. Covarrubias, R. Dominguez, and G. Romero, "Quality of service support for multimedia traffic in mobile networks using a CDMA novel scheduling scheme," *Computers & Electrical Engineering,* vol. 32, pp. 178-192, 2006/01 2006.

[34] W. Yang, J.-Y. Liu, and S.-X. Cheng, "Effect of carrier-frequency offset on the performance of group-orthogonal multicarrier CDMA systems," *Signal Processing,* vol. 86, pp. 3934-3940, 2006/12 2006.

[35] O. C. Ugweje, "Bit error rate performance of multicarrier CDMA system with application to image transmission," *Measurement,* vol. 36, pp. 233-244, 2004/10 2004.

[36] V. Bhaskar and L. L. Joiner, "Performance of punctured convolutional codes in asynchronous CDMA communications under perfect phase-tracking conditions," *Computers & Electrical Engineering,* vol. 30, pp. 573-592, 2004/11 2004.

[37] V. Bhaskar and L. L. Joiner, "Variable energy adaptation for asynchronous CDMA communications over slowly fading channels," *Computers & Electrical Engineering,* vol. 31, pp. 33-55, 2005/01 2005.

[38] J. Wang, B. Zhu, C. Li, C. Sun, and Y. Wan, "Research on multi-objective control algorithm for micro-nano satellite formation based on array signal detection," *Advances in Space Research,* vol. 75, pp. 6342-6352, 2025/04/15/ 2025.

[39] L. V. D A and A. K. C, "Evaluating Supervised Learning Classifier Performance for OFDM Communication in AWGN-Impacted Systems," *Results in Engineering,* vol. 26, p. 105178, 2025/06/01/ 2025.

[40] J. O. Mark, B. B. Samir, and N. M. Saad, "Capacity and error probability performance analysis for MIMO MC DS-CDMA system in η–μ fading environment," *AEU - International Journal of Electronics and Communications,* vol. 67, pp. 269-281, 2013/04 2013.

[41] Y. Jabrane, R. Iqdour, B. A. Essaid, and N. Naja, "BER calculation in DS/CDMA over Rayleigh fading channel with power control error using fuzzy systems," *Communications in Nonlinear Science and Numerical Simulation,* vol. 14, pp. 543-551, 2009/02 2009.

[42] M. Jangalwa and V. Tokekar, "Performance analysis of Selective Mapping and clipping based multicarrier-CDMA system with and without MIMO technique," *AEU - International Journal of Electronics and Communications,* vol. 101, pp. 62-68, 2019/03 2019.

[43] A. Dey and A. Nandi, "Spatial assessment of array antenna based joint SDMA-TDMA architecture for DS-CDMA signals," *AEU - International Journal of Electronics and Communications,* vol. 113, p. 152949, 2020/01 2020.

[44] A. Khalid, F. Rashid, U. Tahir, H. M. Asif, and F. Al-Turjman, "Multi-carrier Visible Light Communication System Using Enhanced Sub-carrier Index Modulation and Discrete Wavelet Transform," *Wireless Personal Communications,* vol. 127, pp. 187-215, 2022/11/01 2022.

[45] V. Bhaskar and L. Joiner, "Variable energy adaptation for asynchronous CDMA communications over slowly fading channels," *Computers & Electrical Engineering,* vol. 31, pp. 33-55, 01/31 2005.

[46] V. Bhaskar, "Distribution and density functions of probability of error over slowly fading channels with diversity combining," *Journal of the Franklin Institute,* vol. 348, pp. 1153-1159, 2011/08 2011.

[47] H. Kasban, E. H. Ali, and H. Arafa, "Diagnosing Plant Pipeline System Performance Using Radiotracer Techniques," *Nuclear Engineering and Technology,* vol. 49, pp. 196-208, 2017/02/01/ 2017.

[48] H. J. Pant, "Applications of the radiotracers in the industry: A review," *Applied Radiation and Isotopes,* vol. 182, p. 110076, 2022/04/01/ 2022.

[49] M. S. El_Tokhy, H. Kasban, and E. H. Ali, "Malfunction diagnosis based on residence time distribution of radiotracer signals in industrial processes using machine learning techniques," *Annals of Nuclear Energy,* vol. 211, p. 110976, 2025/02/01/ 2025.

[50] H. J. Pant, S. Goswami, S. B. Chafle, V. K. Sharma, V. Kotak, V. Shukla*, et al.*, "Investigation of transport of radionuclide in a thermal stratification test facility using radiotracer technique," *Nuclear Engineering and Technology,* vol. 54, pp. 1449-1455, 2022/04/01/ 2022.

[51] T. Teng, "Outage probability and ergodic capacity analysis of satellite–terrestrial NOMA system with mixed RF/mmWave relaying," *Physical Communication,* vol. 57, p. 101998, 2023/04/01/ 2023.